Sudirman, S, Natalia, F, Sophian, A and Ashraf, A

 Pulsed Eddy Current signal processing using wavelet scattering and Gaussian process regression for fast and accurate ferromagnetic material thickness measurement

http://researchonline.ljmu.ac.uk/id/eprint/16828/

Article

Pulsed Eddy Current signal processing using wavelet scattering and Gaussian process regression for fast and accurate ferromagnetic material thickness measurement

Sud Sudirman [a], **Friska Natalia** [b], **Ali Sophian** [c,*], **Arselan Ashraf** [d]

[a] *School of Computer Science and Mathematics, Liverpool John Moores University, Liverpool L3 3AF, United Kingdom*
[b] *Faculty of Engineering and Informatics, Universitas Multimedia Nusantara, Tangerang 15811, Indonesia*
[c] *Department of Mechatronics Engineering, Faculty of Engineering, International Islamic University Malaysia, Selangor 53100, Malaysia*
[d] *Department of Electrical and Computer Engineering, Faculty of Engineering, International Islamic University Malaysia, Selangor 53100, Malaysia*

Abstract Testing the structural integrity of pipelines is a crucial maintenance task in the oil and gas industry. This structural integrity could be compromised by corrosions that occur in the pipeline wall. They could cause catastrophic accidents and are very hard to detect due to the presence of insulation and cladding around the pipeline. This corrosion manifests as a reduction in the pipe wall thickness, which can be detected and quantified by using Pulsed Eddy Current (PEC) as a state-of-the-art Non-Destructive Evaluation technique. The method exploits the relationship between the natural log transform of the PEC signal with the material thickness. Unfortunately, measurement noise reduces the accuracy of the technique particularly due to its amplified effect in the log-transform domain, the inherent noise characteristics of the sensing device, and the non-homogenous property of the pipe material. As a result, the technique requires signal averaging to reduce the effect of the noise to improve the prediction accuracy. Undesirably, this increases the inspection time significantly, as more measurements are needed. Our proposed method can predict pipe wall thickness without PEC signal averaging. The method applies Wavelet Scattering transform to the log-transformed PEC signal to generate a suitable discriminating feature and then applies Neighborhood Component Feature Selection method to reduce the feature dimension before using it to train a Gaussian Process regression model. Through experimentation using ferromagnetic samples, we have shown that our method can produce a more accurate estimation of the samples' thickness than other methods over different types of cladding materials and insulation layer thicknesses. Quantitative proof of this conclusion is provided by statistically analyzing and

---

* Corresponding author.
E-mail address: ali_sophian@iium.edu.my (A. Sophian).
Peer review under responsibility of Faculty of Engineering, Alexandria University.

comparing the root mean square errors of our model with those from the inverse time derivative approach as well as other machine learning models.

1. Introduction

Transmission pipelines in the oil and gas industry are assets that need to be inspected and maintained regularly because pipeline failures may have potentially significant consequences in terms of loss of lives, environmental damage, and high economic costs. These challenges make the process unique in that it necessitates sophisticated pipeline risk assessments, technical know-how, and efficient and cost-effective methods. To overcome these challenges, numerous engineering disciplines are needed including structural monitoring and instrumentation, fracture mechanics, and non-destructive testing, to name but a few [1].

The structural integrity of a pipeline could be compromised by corrosions that occur in the pipeline wall that cause a significant reduction in the pipe wall thickness. During an inspection, the wall thickness of the pipeline needs to be determined to ensure that any variations from the expected value are still within the standard manufacturing tolerances. The process of accurately measuring the pipeline thickness is very challenging when it is covered by insulation and cladding layers. The ability to estimate the pipe wall thickness without the removal of the insulation is very beneficial because such removal lengthens inspection time, increases downtime, and incurs costly replacements of the insulation layer [2].

Pulsed Eddy Current (PEC) is the state-of-the-art Non-Destructive Evaluation (NDE) technique for evaluation of corrosion or wall-thinning in ferromagnetic structures, especially when they are insulated or coated [34]. The wide frequency range of the excitation signals allows them to penetrate to various depths and provide more information about the geometry of the structures being evaluated [5]. The method exploits the relationship between the natural log transform of the measured voltage with the material thickness.

Faster inspection speed, better sensitivity and detection, and cost-effectiveness are imperatively needed in many NDE applications [6–8]. Unfortunately, due to the sensor's signal limitation and the non-homogenous property of ferromagnetic materials, PEC techniques usually require signal averaging to improve its performance [9], which slows down the inspection significantly due to repeated measurements of the same location must be made. With PEC, this is especially true when thicker structures are involved as the pulse has to be wider [7] to give sufficient time for the induced eddy current to diffuse.

In the next section, we will present the problem statement and literature review. This is followed by the description of the proposed methodology and the experimentation and analysis of the experimental results.

2. Problem statement and literature review

In this section, the relationship between the signal produced by a Hall Effect device and the thickness of the material is derived by using existing work in the literature. Hall Effect sensors measure the strength of the magnetic field B. Borrowing the derivation of a mathematical model for the PEC-induced detector coil voltage signal V_C by Huang et. al. [10], the measured voltage can be expressed as the sum of multiple exponentially decaying signals weighted by their amplitude over time:

$$V_C(t) = \sum_{k=1}^{n} b_k e^{-c_k t} \tag{1}$$

where the amplitude parameters, b_i and the decay rate constants c_i, are positive real numbers for all k. The parameter n is a positive integer number that represents the effective order of the model. Its value is determined by the number of coils in the sensor. The value of the voltage signal $V_C(t)$ converges as the value of $n \to \infty$.

Chen and Lei [11] determined the largest time constant τ_1, where $\tau_1 = 1/c_1$ in Eq.(1) as a function of the magnetic permeability μ, the electrical conductivity σ, and the thickness d, of the ferromagnetic plate. This relationship is expressed in Eq. (2).

$$\tau_1 = \frac{\mu \sigma d^2}{\pi^2} \tag{2}$$

Separating that corresponding exponential term (the one that has the largest time constant) from the rest of the terms in Eq.(1) yields:

$$V_C(t) = b_1 e^{-\frac{\pi^2}{\mu \sigma d^2} t} + \sum_{k=2}^{n} b_k e^{-c_k t} \tag{3}$$

This exponential term is the dominant contributor to the signal in the late stage, i.e., when t is much larger than 0. Hence, we can approximate the signal when $t \gg 0$ as:

$$V_C(t)|_{t \gg 0} \approx b_1 e^{-\frac{\pi^2}{\mu \sigma d^2} t} \tag{4}$$

Using the Faraday's Law of electromagnetic induction, we can derive the strength of the magnetic field $B(t)$ that induced the voltage.

$$V_C(t) \frac{B(t)}{dt} \tag{5}$$

Rearranging the equation and considering V_H, the voltage measured by the Hall effect device we then have,

$$V_H(t) = k.B(t) = -\frac{k}{N} \int V_C(t) dt \tag{6}$$

where k is the gain factor. Substituting V_C using Eq.(4) and solving the integral gives us the value of V_H when $t \gg 0$ as:

$$V_H(t)|_{t \gg 0} = \frac{k b_1 \mu \sigma d^2}{N \pi^2} e^{-\frac{\pi^2}{\mu \sigma d^2} t} \tag{7}$$

By taking a natural logarithm of the function, we can express the equation as:

$$\ln(V_H(t)|_{t \gg 0}) \approx -\frac{\pi^2}{\mu\sigma d^2}t + \ln\frac{kb_1\mu\sigma d^2}{N\pi^2} \qquad (8)$$

Taking the derivative of the equation yields:

$$\frac{d\ln(V_H(t)|_{t \gg 0})}{dt} \approx -\frac{\pi^2}{\mu\sigma d^2} \qquad (9)$$

Using this model, the gradient of the measured Hall Effect voltage signal in logarithmic space is estimated to be inversely proportional to the square of the ferromagnetic plate's thickness. However, since in practice the signals will be corrupted by noise, determining the gradient of the signal in logarithmic space at $t \to \infty$ will be practically impossible. Therefore, it needs to be evaluated between the time, t_a, when the non-dominant signals, i.e., those expressed as the second term in Eq.(3), have small but non-negligible contributions [12] and the time, t_b, when the signal-to-noise ratio falls below a certain threshold. In this paper, we subsequently refer to this time window as the *Evaluation Period* (EP).

The accuracy of the estimation of the plate's thickness is affected by the deformation of the straight line in Eq.(8) by the other non-dominant signals and noise. The effect of the other non-dominant signals can be reduced by choosing a larger t_a whereas the effect of the noise can be reduced by choosing a smaller t_b. Performing this simultaneously will result in a narrow EP that can result in a less accurate gradient estimation.

As indicated above, the long decay part of the signal can be used to predict the thickness of the specimen under test. Based on this, many feature extraction techniques for thickness prediction have been developed, such as those reported in [13–15]. However, the accuracy of the thickness prediction when the feature is extracted is affected by the noise in the signal. Consequently, PEC systems and techniques that have been reported typically use signal averaging to reduce the noise in their sensing device's output signals. Examples of such systems are reported in [16–19], where a minimum of 10 signals are used in the averaging. Huang et al [20] also suggested the use of signal averaging for denoising noise in the PEC signals in addition to the application of a median filter. The disadvantage of the use of signal averaging is that the time needed for each measurement will be increased significantly as multiple cycles have to be acquired for each measurement point [15,21], and as a result, the speed of inspection will be lowered. This is especially undesired when the area of the specimen to be tested is large and/or a fast scanning is required. The scanning speed can be improved if only a single pulse is required for each measurement. The use of Gaussian process regression (GPR), instead of line fitting of the signal's decay, has been presented for improving the performance of the measurement when a Hall device was used as the sensing device and the averaging of signals is used [21]. Thanks to the generally smaller detecting cross-section areas, magnetic sensors offer the advantage of better spatial resolution over sensing coils, which may make them the preferred solution in some applications despite PEC systems mostly using detector coils.

It is also worth noting that our proposed method is different from other feature-extraction-based approaches for PEC NDT in the literature, such as [22,23] where Principal Component Analysis (PCA) and Hilbert transform were used, respectively. First, in this research, we used ferromagnetic sample material whereas, in the other papers, non-magnetic

(aluminum) sample materials were used. The consensus in the literature suggests that the magnetic permeability of the samples under consideration affects the characteristics of the resulting PEC signals and therefore, the type of signal processing technique to use. Secondly, the feature-extraction techniques in those papers were applied to the differential of the PEC signal, which is obtained by subtracting the testing sample response signal from the reference signal. In this paper, on the other hand, we apply the feature extraction technique on the natural log transform of the normalized PEC signal to utilize the strong relationship between the gradient of the measured voltage signal in logarithmic space and the square of the plate's thickness as derived in Eq. (1) to (9). For speeding up PEC measurements, the use of an array or a matrix of sensors has been proposed [7,9]. The main drawbacks of the use of a sensor array are the complexity of the system and the manufacturing cost involved. A fast crack profile reconstruction method using transient slices and spectral components of PEC signals has been proposed in [24], however, this method was developed for crack estimation of non-ferromagnetic materials, rather than for corrosion or wall loss estimation of ferrous materials.

3. Methodology

Our approach to solving the problem of getting an accurate estimation of a ferromagnetic material sample thickness without having to obtain a large number of measurements is elucidated as a flowchart in Fig. 1. The proposed method uses several signal processing and machine learning techniques that eventually lead to the development of a regression model that fits a set of discriminating features derived from the measured PEC signals of known material thickness. The main stages of the process are described in the remainder of this section.

3.1. Data Pre-Processing

Upon the acquisition of the PEC signals of a given material thickness, a median filter is applied to remove any outliers in the measurements that can occur due to measurement or instrumentation errors. The process is carried out in the time domain in overlapping windows of a pre-determined width, w_{mf}, over the entire length of the signal. The filtered signal is obtained by placing the median of the values in the input window, at the location of the center of that window. Median filter is chosen because this filter is widely used in other PEC-based signal processing techniques in the literature [9,20].

To reduce the effect of insulation layer thickness variations, we employ the normalization technique as suggested in [25]. The signal data are normalized to the [0 1] range by subtracting the mean of their lowest values and dividing the results by the mean of their highest values. Since we will be working with the data in the logarithmic space, we also need to cap the minimum value to a small positive value. We then determine the time when the signal just drops below a certain threshold and remove any data prior to this time, hence effectively setting the time at that location to be the origin. We then determine the t_a and t_b that mark the start and end of EP by inspecting the logarithmic plot of the data.
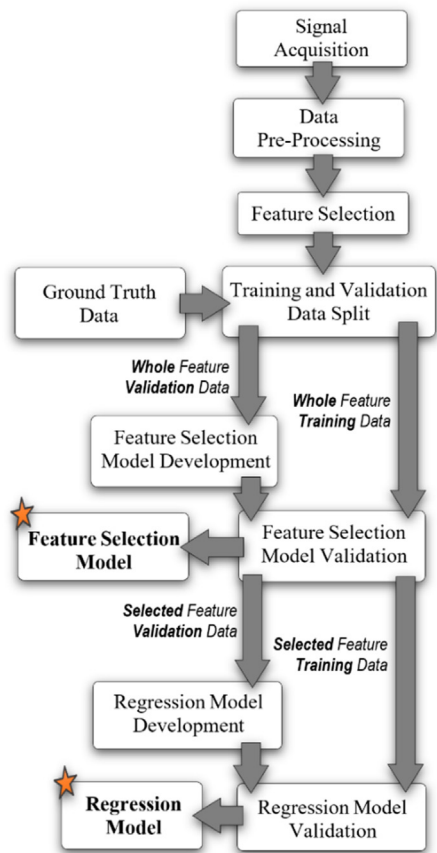
Fig. 1 Overview of the proposed methodology. The two outputs, the Feature Selection model and the Regression model, will be used in estimating the sample thickness.

3.2. Feature calculation using wavelet scattering

The choice of features is a crucial step in machine learning. It can significantly affect the performance of the model that is developed. A good feature must capture as much as possible all relevant and discriminating information that is inherent in the data in as few dimensions as possible. We have selected wavelet scattering as the technique to generate such a feature for the PEC signal data.

Wavelet scattering of time series data generates a set of features that is invariant to translation and is stable to deformations. The method also does not require training and can work well with a small amount of data. The technique allows time–frequency analysis of non-stationary data, which is an advantage over Fourier analysis, the canonical signal analysis technique in the past few decades.

As is previously shown in Eq.(8), the gradient of the measured signal in natural logarithm space is inversely proportional to the square of the material thickness. Other factors in the measurements, such as lift-off distances, insulation layer thickness, and types of the cladding material, will affect the bias component of the equation. Measurement noise, while is present equally throughout the measurement period, will have different amplitudes at different times in the log space. Wavelet scattering transform of the natural logarithm of the signal should provide the discrimination of the types of deformations, separation of the deformation factors, and invariance to bias that we need.

To illustrate this, let's denote the wavelet scattering transform of a time series signal x_t as $\Phi(x_t)$. It is shown that wavelet scattering transform is invariant to translation [26], hence $\Phi(x_t) = \Phi(x_{t+T})$, where x_{t+T} is a time-shifted variant of x_t by T. In a linear system $x_t = mt + b_x$, (where m and b are the gradient and bias, respectively), it can easily be shown that another linear system of the same gradient $y_t = mt + b_y$ as a time shifted variant of x_t by $(b_y - b_x)/m$. By that reasoning, the wavelet scattering features of the signal having different bias values should be similar.

Wavelet scattering is also shown to be Lipschitz continuous to deformations [26]. For Lipschitz constant C greater than 0 and a displacement field τ_u causing a deformation to x_t that creates $\tilde{x}_t$, it is shown that:

$$\|\Phi(x_t) - \Phi(\tilde{x}_t)\| \leq \sup_u(|\nabla \tau_u|)C \int \|x_u\|^2 du \qquad (10)$$

This means the change in magnitude of the features that represent the elements of the signal affected by the deformation should correspond linearly to the magnitude of the deformation itself. Therefore, if such a deformation is responsible for the variation in the gradient of the signal, that will be reflected linearly in the wavelet scattering coefficients.

A wavelet scattering of a one-dimensional signal x for a maximum scale factor of 2^J works by iteratively convolving the signal with a bank of Morlet wavelets $\{\psi_{j,k}\}$ and then taking their modulus. The parameters j and k denote the scattering stage and the wavelet number, respectively and such that $0 \leq j \leq J$ and $1 \leq k \leq K_j$, where K_j is the maximum number of wavelets in the jth stage.

The output of the wavelet convolution and modulus in each stage j becomes the input of the next. At each stage, the results are convolved with a scaling function ϕ_J which acts as a data averaging process to produce that stage's scattering coefficients S_j. To start with, x is not convolved with any wavelets. The scattering coefficient at this level, S_0, is simply $x * \phi_J$. That scattering coefficient is also known as the zeroth-order scattering coefficient. At each of the subsequent stages, the following steps take place:

1. The wavelet transform is applied to the output of the previous stage using each wavelet in the wavelet bank.
2. The modulus of each transformed output is taken. This result will be used as the input to the next stage.
3. The result is also averaged by convolving with the scaling function to produce a set of scattering coefficients of that stage $\{S_j\}$.

These sets of scattering coefficients are the feature that we obtained as the product of this wavelet scattering transform.

3.3. Feature reduction using Neighborhood Component feature Selection (NCFS)

The dimension of the feature produced by the wavelet scattering transform is typically very high. Prior to using the feature in machine learning, it is therefore important to select a small subset of the feature that captures most information about the underlying data and discard others that are irrelevant or redundant. This process effectively reduces the dimensions of features which will improve the machine learning model that

is developed. The model will have better generalization performance, i.e., the ability to estimate a good outcome on unseen input. The model will also be smaller, leaner, and computationally faster because it does not have a high requirement for memory size and computational power to compute and store large numbers of features.

For this, we decided to use the Neighborhood Component Feature Selection (NCFS) algorithm [27] to perform the dimensionality reduction process. This is a supervised feature reduction method with the goal of maximizing the prediction accuracy of regression and classification algorithms compared to unsupervised methods such as PCA [22] whose aim is to preserve as much variance in the reduced data as possible. The method is also non-parametric, i.e., making no assumptions about the shape of the class distributions or the boundaries between them; hence, is suitable for our thickness prediction problem.

The NCFS method assigns a weight to each dimension of the feature as a measure of that dimension's importance. The higher the weight, the more important that dimension of the feature is in determining the correct response. The method is essentially a nearest-neighbor-based feature weighting method. It uses the gradient ascent technique to maximize the expected leave-one-out classification accuracy with a regularization term. The leave-one-out method attempts to maximize the probability of correctly predicting the response of an input variable, by analyzing the other input variables and their correct responses. The method applies regularization with parameter λ whose purpose is to reduce the chance of overfitting. The chance of overfitting is affected by the number of observations. If we have only a small number of observations, the chance of overfitting increases, and as a result higher regularization parameter value is desirable. To get the best value for λ, we split the data into training and validation sets using cross-validation method and apply NCFS on the training set using several values of λ in the $[\lambda_{\min} \ \lambda_{\max}]$ range. The best λ value is one that minimizes the average loss across the cross-validation folds.

Once the best λ value has been determined, we sort the feature according to its assigned weights and select the top few features to be used for training regression models in the subsequent stage.

3.4. Thickness estimation using Gaussian process regression

The thickness prediction is performed via regression analysis of the relationship between the selected wavelet scattering feature as an independent variable with the material thickness as its dependent variable. There are several machine learning regression models that can be used, each has advantages and disadvantages over others, and some are more suitable for a certain type of applications and requirements than others. Our review of the literature in the field of regression analysis suggests that Gaussian Process Regression (GPR) [28] fits well to our need of a) being able to provide uncertainty measurement on the resulted prediction and b) providing relatively good performance using a small number of training data.

As the name suggests, GPR is a supervised machine learning algorithm that uses a Bayesian approach to solve the regression problem between a set of input variables x and its outputs y. Let's express the relationship between the input

and output variables as a general function involving a parameter w, e.g., $y = wx + \epsilon$ for a linear function. Within a limited input space, GPR works by a) coming up with a prior distribution $p(w)$ and b) using Bayes' rule to relocate the probabilities based on some observed data X and come up with a posterior distribution $p(w|y, X)$. To get a prediction y^* at some previously unobserved input x^*, GPR develops a predictive distribution $p(y^*|x^*, y, X)$ using all possible predictions of w weighted by its posterior distribution.

$$p(y^*|x^*, y, X) = \int_w p(y^*|x^*, w)p(w|y, X)dw \tag{11}$$

In practice, the prior and likelihood are assumed to be Gaussian for the integration to be tractable hence the point prediction can be calculated using the mean prediction and its covariance. Furthermore, the technique can also incorporate independent-and-identically distributed Gaussian noise, $\epsilon \ N(0, \sigma^2)$ to the predictions by summing the predictive distribution and noise distribution.

GPR offers several advantages namely:

- Ability to use the predictions to interpolate observations,
- Ability to directly compute confidence intervals due to the probabilistic nature of the predictions, and
- Allows some flexibilities e.g., using different covariance functions (kernel) and specifying noise distribution σ.

The technique is considered very efficient on a small dataset and small input dimension but loses its efficiency in high dimensional spaces, i.e., when the number of features exceeds a few dozens. This problem is alleviated in our case since we apply NCFS to the wavelet scattering feature to reduce the feature dimension prior to it being used in GPR.

4. Experimental setup

We conducted an experiment to empirically assess the suitability of the proposed methodology in estimating the thickness of material using a single observation of the PEC signal. We built a PEC system and connected it to a PC that samples and records the signals as our raw data. The data is split into training and test sets, where the training set is used to build the models as illustrated in Fig. 1 and the test set is used to evaluate the performance of the models, as shown in Fig. 2, and analyze the effectiveness of the overall approach.

4.1. PEC system building and signal acquisition

We built a PEC-NDT system consisting of a probe, a data acquisition, and a laptop running LabVIEW software as illustrated in a block diagram shown in Fig. 3.

The design of our PEC-NDT system takes into account the findings of a study [25] on Lift-Off Invariance (LOI). The three findings of that study that are most relevant to our case are as follows:

1. LOI points exist in PEC systems whether using coils or magnetic sensors for inductive voltages or magnetic field measurement. For a Halls device, the point can be found
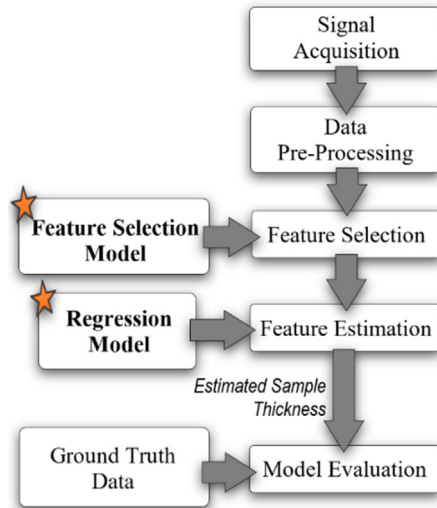
Fig. 2 Overview of the strategy to evaluate the accuracy of the estimated sample thickness produced using the developed Feature Selection and Regression models.
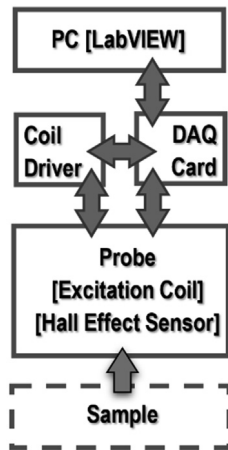

Fig. 3 The PEC-NDT system block diagram.

as the crossing of two first-order derivatives of the magnetic field signals against time for two different lift-offs when plotted in the time domain.

2. For variable lift-off, multiple LOI points can be found. These points define a range in which the LOI changes as the lift-off varies. Two metrics are used to measure the quality of LOI namely LOI-Range Width and LOI-Range Center, where the smaller the LOI-Range Width is and the larger the LOI-Range Center is, the better. The study finds that placing the Hall sensor at the center of the probe produces the best result.

3. The study also found that the LOI is closely related to the conductivity of the samples under inspection.

Based on the above, five design decisions of our PEC-NDT system are made. They are:

1. A Hall Effect sensor is used instead of a coil to reduce the overall size of the PEC-NDT device. This should allow the device to better touch the pipe surface hence reducing the occurrence of lift-off.

2. The dimension of the Hall sensor we used is a lot smaller than the inner diameter of the excitation coil.

3. The Hall sensor is placed exactly at the center of the excitation coil.

4. We used two types of materials for cladding with very different values of conductivity.

5. We incorporate an insulation layer on top of the sample and vary its thickness. By varying the insulation thickness in our experiment, we also simulate variations in lift-off values.

The probe consists of an excitation coil and a Hall Effect sensor (DRV5053VA) whose sensitivity is 90 mV/G. A ferrite core is used for concentrating the magnetic flux and strengthening the Hall device's output signal. The inner and outer diameters of the exciter coil are 100 mm and 110 mm, respectively. The coil has 200 turns and has an effective height of 6 mm. A MOSFET was used to switch on and off high excitation currents with a pulse width of 25 ms driven to the excitation coil. The signal is detected by the Hall-effect device, sent to the PC through a DAQ card which samples it at 20,000 samples per second. Fig. 4(a) shows the cross-sectional illustration of the sample and excitation coil with their measurements, while Fig. 4(b) shows a picture of the experimental setup, which includes the PEC system.

Four square carbon steel S50C plates with different thicknesses with surface dimensions of 300 mm × 300 mm are used as samples. The samples have four thickness variations which are 9.12, 10.02, 11.06, and 12.08 mm, and are uniform across the sample's volume. Two different materials were used for the cladding, namely aluminum (grade 1100) and stainless steel (grade 304). Both of them are non-ferromagnetic. The thickness of the cladding for both materials is fixed at 0.5 mm. A layer of non-conductive material, which simulates the insulation layer, is inserted between the sample and the cladding. Five different values of insulation layer thickness are used in the experiment which are 3.0, 5.0, 8.0, 10.0, and 13.0 mm. This results in twenty different combinations of sample thickness and insulation layer thickness. For each combination, 50 different PEC signals, sampled at a rate of 20 KS/s, are recorded – resulting in a total of 1000 observations, or 250 observations per sample thickness, in a form of time series data, for each cladding material type.

4.2. Data Pre-Processing

We applied a median filter to the signal. The width of the overlapping window w_{mf} is set to 100. We find this value to be the best in providing good a balance between maintaining the signal's overall shape, and noise and outliers removal. Following the data normalization step as described in the previous section to make the signal value in the range of [0 1], we remove the first part of the signal where it is stationary. We mark a time in the signal where the signal drops to and below 0.98 and discard all data prior to that time. To determine the values of t_a and t_b that mark the start and end of EP, we plot the average of the normalized signals for each combination of sample thickness, insulation layer thickness, and cladding material type on a semi-logarithmic scale. Four examples of such a plot are shown in Fig. 5. The plots in the left column are at a fixed insulation layer thickness of 3 mm whereas those in the right
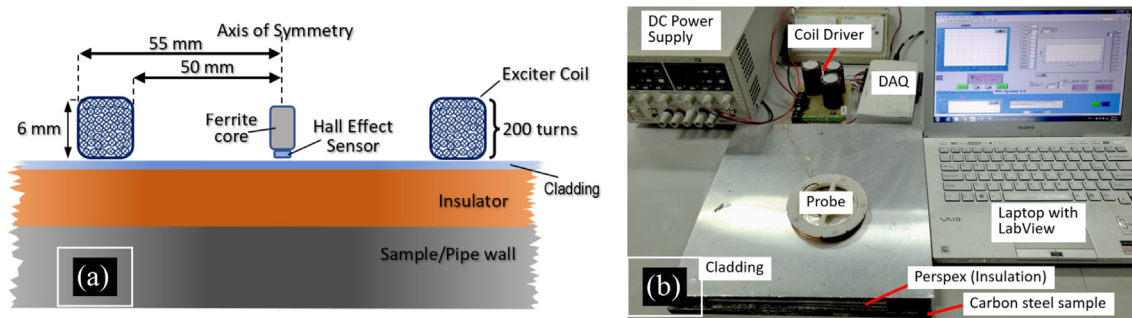
Fig. 4 (a) Cross-sectional illustration of the sample and excitation coil (drawn not to scale); (b) Picture of the experimental setup.
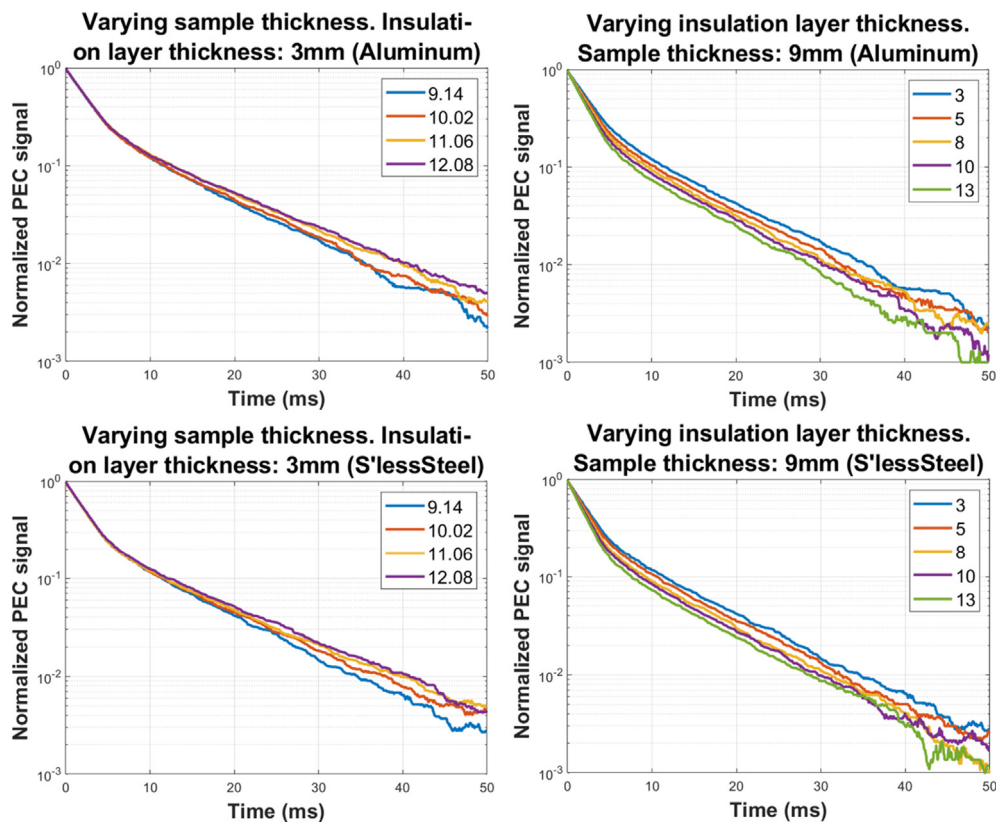

Fig. 5 Plots of the normalized PEC signals on a semi-logarithmic scale at varying sample thickness when the insulation layer thickness is fixed at 3 mm (left column), and at varying insulation layer thickness when the sample thickness is fixed at 9 mm (right column) for both types of cladding material.

column are at a fixed sample thickness of 9.12 mm. The plots for aluminum and stainless steel cladding material are shown in the top and the bottom row, respectively. After inspecting all the plots, we decide the values of the t_a and t_b time marks to be 10 and 35 ms, respectively. They are determined by visually identifying parts of the signal that have roughly a constant rate of decay in semi-logarithmic space.

4.3. Feature calculation and reduction

At this stage, each of the 1000 observations has a length of 499 points. Before calculating the features, we apply a natural log transform to the data. We then calculate the features using wavelet scattering transform by setting the maximum number of stages J as 2, and K_1 and K_2 are 8 and 1, respectively. This results in a 576-dimension feature for each observation.

The data is then split into two sets, a training set A_{TRAIN} and a test set A_{TEST} with a ratio of 9:1. The training set is then further divided using the kfold method into two more sets, A'_{TRAIN} and A_{VAL}, which are the sub-training set and validation set, respectively. The value of k is set to 5. We find the best λ value for the NCFS between $\lambda_{\min} = 0$ and $\lambda_{\max} = 0.11$ in 20 increments by selecting λ that yields the lowest mean loss across all five cross-validations. This is found to be 0.0058 for both types of cladding material. We proceed by applying NCFS with the chosen λ to all wavelet scattering features in

A_{TRAIN} set and obtain a weight value for each of the 576 elements of the feature. We then sort the feature according to their weights and select N_f number of feature elements that have the highest weights to represent the entire 576-dimension feature. We describe the process to decide the value of N_f in the next section.

4.4. Thickness estimation process

The relationship between the selected features and their expected responses is to be modeled using a Gaussian process regression. Like most other machine learning models, the GPR model has several hyperparameters, which are essentially internal values that need to be tuned to control the way the model training process works. In this implementation, we employ an automatic process to optimize these hyperparameters by using Bayesian optimization and cross-validation. The process starts by training the model using a set of hyperparameter values and evaluating the model performance using an objective function. The estimate for the next best set of hyperparameter values to use is obtained using an acquisition function. This is a mathematical function that combines the predicted mean and predicted variance, obtained from evaluating the model performance, into a criterion that will direct the search.

In practice, before training the GPR model the training set A_{TRAIN} is again split using kfold into a sub-training set and a validation set. Though this time, the sets contain the reduced-length features as opposed to full-length features in the previous step. The value of k is set to 5. During training, the hyperparameter optimization seeks to minimize the log-transformed objective function, $\log(1 + loss)$, where $loss$ is the cross-validation mean squared error, with the Expected-Improvement function [29] set as the acquisition function used to search the hyperparameter space. We set the noise distribution σ as the only hyperparameter in this case. Once the best σ value is found, the model is then trained using the entire training set A_{TRAIN}. The data in the test set A_{TEST} are then passed on to the workflow shown in Fig. 2 to evaluate the trained model's performance.

5. Experimental results and analysis

5.1. Thickness estimation results

The experiment is repeated 20 times, each using a different set of 100 randomly selected observations from the 1000 observations as the test set. We also experimented with using different values of N_f ranging from 1 to 11 to find one that gives the lowest average Root Mean Square Error (RMSE) on the test set. Using the results, as shown in Fig. 6, we concluded that the best values for N_f are 3 and 5 for Aluminum and Stainless-Steel cladding case, respectively. Using these values, we then proceed with analyzing the performance of the models by comparing the results with other machine learning models and approaches.

5.2. Results analysis and discussion

We implemented the proposed method and record the predicted thickness values and compare them to the actual thickness values. We use RMSE as the metric to assess the performance of the proposed method. We also implemented other methods to allow us to provide a qualitative comparison of the proposed method. Subsequently, we denote the results of our proposed method as GP.

The first comparative method is the Inverse Time Derivative (ITD), or $|\nabla|^{-1}$ method proposed in [19]. This method is based on a mathematical model that is analytically derived from the relationship between the thickness of the material and the pulse signal. We showed parts of this derivation in our literature review section, i.e., Eq. (1)-(8). This method relies on averaging several pulse signals in order to reduce the noise and obtain a more accurate determination of the time derivative. To show the validity of applying the same method to our data, we plot the average of the normalized PEC signal in the logarithm domain for each sample thickness value and insulation layer thickness value in the left and right columns of Fig. 7, respectively. Each line in the left column diagrams represents the average signal over all insulation layer thickness
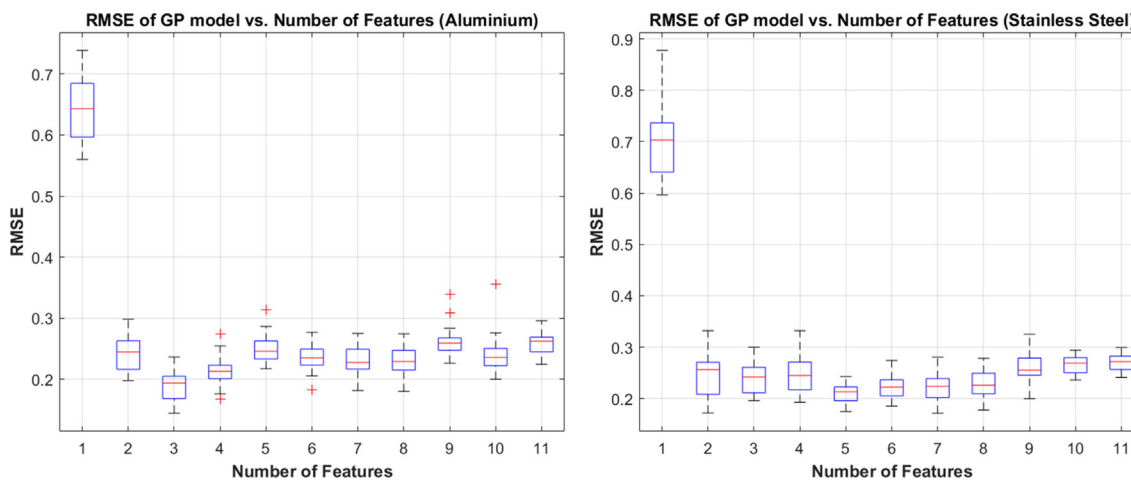

Fig. 6 A box plot of the RMSE of the measured sample thickness (Aluminum) from 20 experiments using the first eleven values of N_f. The best number of elements is three.
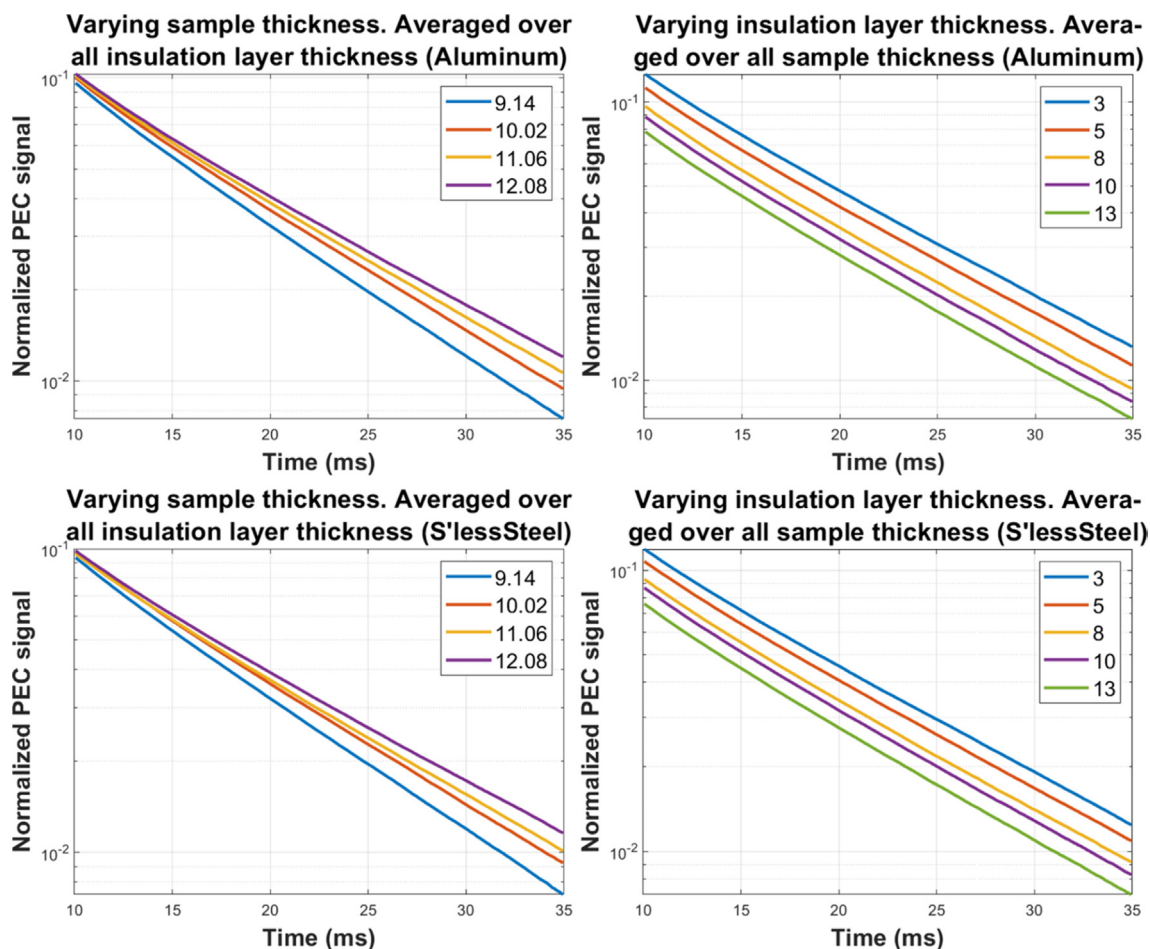
Fig. 7 Plots of the averaged normalized PEC signal inside the Evaluation Period on a semi-logarithmic scale at varying sample thickness values (left column), and varying insulation layer thickness values (right column) for both types of cladding material.

values and is calculated from 250 observations. Each line in the right column diagrams, on the other hand, represents the average signal over all sample thickness values and is calculated from 200 observations. The diagrams in the top and bottom rows correspond to aluminum and stainless steel cladding material data, respectively.

As can be seen from the figure, the plots are generally linear with their gradients being affected by the sample thickness and are insensitive to the insulation layer thickness values as suggested by the mathematical model. This observation also proves that our data still has the properties described in [19] hence the ITD method described in that paper should be applicable in this case.

In practice, however, taking the average of a large number of observations is not practical since it will considerably increase the inspection time. Therefore, for the purpose of performance comparison in this experiment, we average only five observations before calculating the inverse time derivative feature used to fit the quadratic regression model. In subsequent discussion and analysis, we denote this method with its abbreviation as ITD.

As the second comparative method, we develop a GP regression model without using the wavelet scattering and feature selection processes. The feature, in this case, is an 11-point sampled log-transformed normalized signal, similar to the one

suggested in [30]. The eleven points are spread equally between the t_a and t_b time marks that mark the start and end of EP. We denote this method as GPX. In addition, we also develop other regression models, ranging from the simplest ones such as Linear Regression, Kernel Regression, and Binary Regression Tree [31 32], to Support Vector Machine (SVM) Regression [33] to LSBoost [34] on an ensemble of weak regression trees. The workflow to develop these regression models is identical to the one used to develop the proposed method, i.e., the models are trained using features that are the result of wavelet scattering and NCFS processes.

As mentioned previously, the experiment is repeated 20 times, each using a different set of 100 randomly selected observations from the 1000 observations as the test set. The mean RMSE of the predictions using all the models is presented in Table1. As can be seen from the table, our method produces the smallest RMSE for both cladding material types.

To provide a more complete picture of the relative performance of our proposed method compared to the others, we also show the box plot of the results in Fig. 8. The figures show the minimum, median, maximum, and first and third quartiles of RMSE of the models.

We employ a null hypothesis test to determine the statistical significance of the difference in the performance of our proposed method compared to other approaches and machine

Table 1 Averaged RMSE Of The Proposed Method And Other Approaches. The Top And Bottom Numbers Correspond To Aluminum And Stainless Steel Results, Respectively.

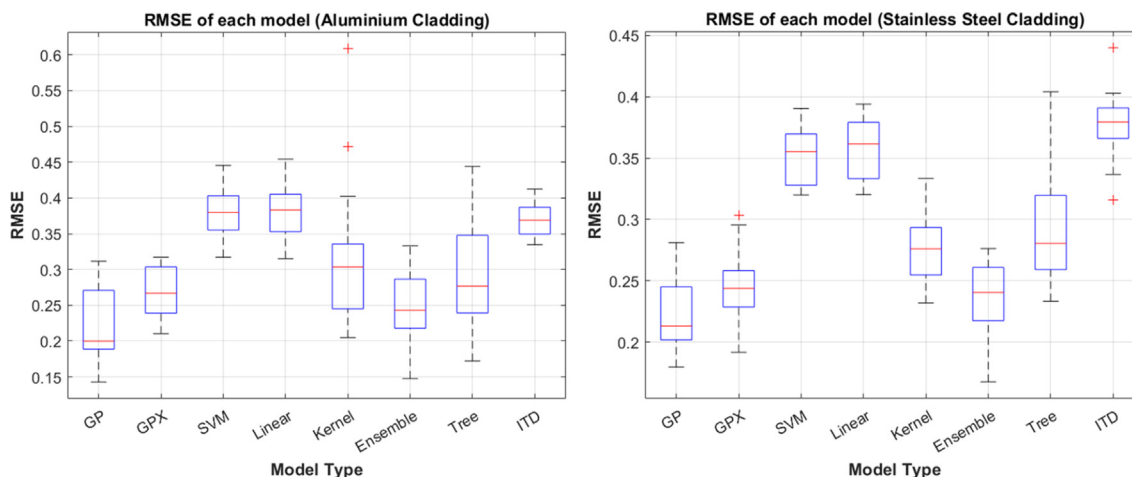| GP	GPX	SVM	Linear	Kernel	Ensemble	Tree	ITD
0.221	0.267	0.378	0.381	0.312	0.248	0.296	0.370
0.222	0.245	0.353	0.358	0.275	0.237	0.294	0.378

Fig. 8 Box plot comparing the performance over 20 experiments of the proposed method with other approaches and machine learning models.

Table 2 Statistical analysis of other methods' and models' performance when compared to the proposed GP method (Aluminum).

Model	Normal Distribution?	Similar Variance?	Statistically Similar?	Hypothesis test used
GP	Yes (0.20)	N/A	N/A	N/A
GPX	Yes (0.72)	Yes (0.09)	No (<0.05)	t-test
SVM	Yes (0.99)	Yes (0.13)	No (<0.05)	t-test
Linear	Yes (0.99)	Yes (0.22)	No (<0.05)	t-test
Kernel	Yes (0.34)	No (<0.05)	No (<0.05)	Welch's
Ensemble	Yes (0.82)	Yes (0.66)	Yes (0.09)	t-test
Tree	Yes (0.61)	Yes (0.15)	No (<0.05)	t-test
ITD	Yes (0.93)	No (<0.05)	No (<0.05)	Welch's

Table 3 Statistical analysis of other methods' and models' performance when compared to the proposed GP method (Stainless Steel).

Model	Normal Distribution?	Similar Variance?	Statistically Similar?	Hypothesis test used
GP	Yes (0.44)	N/A	N/A	N/A
GPX	Yes (0.87)	Yes (0.85)	No (<0.05)	t-test
SVM	Yes (0.71)	Yes (0.46)	No (<0.05)	t-test
Linear	Yes (0.91)	Yes (0.61)	No (<0.05)	t-test
Kernel	Yes (0.99)	Yes (0.85)	No (<0.05)	t-test
Ensemble	Yes (0.85)	Yes (0.62)	Yes (0.12)	t-test
Tree	Yes (0.60)	No (<0.05)	No (<0.05)	Welch's
ITD	Yes (0.90)	Yes (0.78)	No (<0.05)	t-test

learning models. The type of null hypothesis test used depends on whether the distribution of the two sets of results under comparison follows a normal distribution and whether they have similar variances. We use the Kolmogorov-Smirnov test [35] to check the former and the Bartlett's test [36] to confirm the latter. If the two sets of results under comparison follow a normal distribution and have similar variances, then the two-tailed t-test is used, otherwise, the two-tailed two-sample Welch's t-test [37] is used. The statistical analysis of the results is given in Table 2 and Table 3. The second column in the tables shows the result of the Kolmogorov-Smirnov test, the third column shows the result of the Bartlett's test, and the

Table 4 The summary of the statistical test results. Positive ∆mRMSE means that the proposed method has lower RMSE than the corresponding approach/machine learning model.

Model	Aluminum		Stainless Steel	
	∆mRMSE	Statistically significant?	∆mRMSE	Statistically significant?
GPX	0.046	Yes	0.023	Yes
SVM	0.157	Yes	0.131	Yes
Linear	0.160	Yes	0.136	Yes
Kernel	0.091	Yes	0.053	Yes
Ensemble	0.027	No	0.015	No
Tree	0.074	Yes	0.072	Yes
ITD	0.149	Yes	0.156	Yes

fourth column shows the result of the two-tailed t-test comparing the distribution with the proposed GP method. The type of t-test used is shown in the fifth column. The numbers in brackets are the p-value of the respective test result.

The summary of the statistical test results is provided in Table 4. The results show that our method has consistently lower RMSE than all other methods and machine learning models. The improvement ranges from 0.015 to 0.160. Our experiment has also shown that these improvements are statistically significant in all but one model, namely the ensemble of weak regression trees using the LSBoost technique.

The proposed method can significantly improve the inspection speed depending the pulse frequency used. For example, when the pulse frequency is 10 Hz, for the conventional ITD method, 1 s is required to obtain 10 repeated measurements. With the new proposed method, only 100 ms is required for the data acquisition and the performance is also better in RMSE. As the data acquisition is taking most of the inspection time, it can be safely said that the new method will cut the inspection time by 90% without sacrificing the performance.

6. Conclusion

We have developed a machine-learning-based method to predict ferromagnetic sample thickness using the Pulsed Eddy Current non-destructive testing technique. Our method applies Wavelet Scattering transform to the log-transformed PEC signal to generate a suitable discriminating feature and then applies Neighborhood Component Feature Selection method to reduce the feature dimension before using it to train a Gaussian Process regression model. This approach has several advantages over other state-of-the-art PEC NDT approaches. First, it removes the need of taking multiple measurements of the PEC signals and calculating their average to reduce the effect of measurement noise and bring the prediction accuracy up to an acceptable level. We have shown through statistical analysis of experimental results that our method produces a lower average root mean square error than other comparable methods over twenty repeats of the experiment. We also have shown that these improvements are statistically significant in all but the ensemble of weak regression trees with the LSBoost technique. Additionally, our proposed method is lightweight since the feature reduction technique that we apply before training the regression model will produce a smaller model making it deployable on a portable device, hence suitable for an in-situ pipeline inspection. On the other hand, our method

shares a similar set of disadvantages with other machine learning-based approaches, which is requiring many data and a capable high-spec computer for model training. In our future work, we will apply this technique to PEC signals that are produced using different types of sensors to assess the technique's generalizability as a PEC-NDT solution.

Declaration of Competing Interest

References

[1] R.W. Motriuk, "Pipeline Structural Integrity", in *Encyclopedia of Life Support Systems*, Alberta, UNESCO-EOLSS, Canada, 2012.

[2] A. Sophian, G. Tian, M. Fan, Pulsed Eddy Current Non-destructive Testing and Evaluation: A Review, Chinese J. Mech. Eng. 30 (3) (2017) 500–514, https://doi.org/10.1007/s10033-017-0122-4.

[3] Z. Xu, X. Wu, J. Li, Y. Kang, Assessment of wall thinning in insulated ferromagnetic pipes using the time-to-peak of differential pulsed eddy-current testing signals, NDT E Int. 51 (Oct. 2012) 24–29, https://doi.org/10.1016/j.ndteint.2012.07.004.

[4] Y. Fu, P.R. Underhill, T.W. Krause, Factors Affecting Spatial Resolution in Pulsed Eddy Current Inspection of Pipe, J. Nondestruct. Eval. 39 (2) (2020) 34, https://doi.org/10.1007/s10921-020-00679-0.

[5] J. García-Martín, J. Gómez-Gil, E. Vázquez-Sánchez, Non-destructive techniques based on eddy current testing, Sensors 11 (3) (2011) 2525–2565, https://doi.org/10.3390/s110302525.

[6] J. Padiyar M. *et al.*, Fast, Accurate, and Reliable Detection of Damage in Aircraft Composites by Advanced Synergistic Infrared Thermography and Phased Array Techniques. Appl. Sci. vol. 11, no. 6. 2021, 10.3390/app11062778.

[7] G. Piao, J. Guo, T. Hu, Y. Deng, H. Leung, A novel pulsed eddy current method for high-speed pipeline inline inspection, Sensors Actuators A Phys. 295 (2019) 244–258, https://doi.org/10.1016/j.sna.2019.05.026.

[8] B. Purna Chandra Rao, "Non-destructive Testing and Damage Detection BT - Aerospace Materials and Material Technologies : Volume 2: Aerospace Material Technologies," in *Aerospace Materials and Material Technologies*, N. E. Prasad

and R. J. H. Wanhill, Eds. Singapore: Springer Singapore, 2017, pp. 209–228.

[9] C. Huang, W. Xinjun, X. Zhiyuan, Y. Kang, Pulsed eddy current signal processing method for signal denoising in ferromagnetic plate testing, NDT E Int. 43 (7) (2010) 648–653, https://doi.org/10.1016/j.ndteint.2010.06.010.

[10] C. Huang, X. Wu, Z. Xu, Y. Kang, Ferromagnetic material pulsed eddy current testing signal modeling by equivalent multiple-coil-coupling approach, NDT E Int. 44 (2) (Mar. 2011) 163–168, https://doi.org/10.1016/j.ndteint.2010.11.001.

[11] X. Chen, Y. Lei, Excitation current waveform for eddy current testing on the thickness of ferromagnetic plates, NDT E Int. 66 (Sep. 2014) 28–33, https://doi.org/10.1016/j.ndteint.2014.04.006.

[12] Z. Su, S. Ventre, L. Udpa, A. Tamburrino, Monotonicity based imaging method for time-domain eddy current problems, Inverse Probl. 33 (12) (2017) 125007, https://doi.org/10.1088/1361-6420/aa909a.

[13] N. Ulapane, A. Alempijevic, J. Valls Miro, T. Vidal-Calleja, Non-destructive evaluation of ferromagnetic material thickness using Pulsed Eddy Current sensor detector coil voltage decay rate, NDT E Int. 100 (2018) 108–114, https://doi.org/10.1016/j.ndteint.2018.08.003.

[14] W. Cheng, Pulsed eddy current testing of carbon steel pipes' wall-thinning through insulation and cladding, J. Nondestruct. Eval. 31 (3) (2012) 215–224, https://doi.org/10.1007/s10921-012-0137-9.

[15] L. Nguyen, N. Ulapane, J.V. Miro, G. Dissanayake, F. Munoz, Improved signal interpretation for cast iron thickness assessment based on pulsed eddy current sensing, in: in 2017 12th IEEE Conference on Industrial Electronics and Applications (ICIEA), 2017, pp. 2005–2010, https://doi.org/10.1109/ICIEA.2017.8283167.

[16] N. Ulapane and L. Nguyen, "Review of pulsed-eddy-current signal feature-extraction methods for conductive ferromagnetic material-thickness quantification," Electron., vol. 8, no. 5, 2019, 10.3390/electronics8050470.

[17] C. Huang, X. Wu, An improved ferromagnetic material pulsed eddy current testing signal processing method based on numerical cumulative integration, NDT E Int. 69 (Jan. 2015) 35–39, https://doi.org/10.1016/j.ndteint.2014.09.006.

[18] A. Sophian, G.Y. Tian, D. Taylor, J. Rudlin, Design of a pulsed eddy current sensor for detection of defects in aircraft lap-joints, Sensors Actuators, A Phys. 101 (1-2) (2002) 92–98.

[19] F. Nafiah, M.O. Tokhi, S. Majidnia, J. Rudlin, Z. Zhao, F. Duan, Pulsed Eddy Current: Feature Extraction Enabling In-Situ Calibration and Improved Estimation for Ferromagnetic Application, J. Nondestruct. Eval. 39 (3) (2020), https://doi.org/10.1007/s10921-020-00699-w.

[20] C. Huang, W. Xinjun, X. Zhiyuan, Y. Kang, Pulsed eddy current signal processing method for signal denoising in ferromagnetic plate testing, NDT E Int. 43 (7) (Oct. 2010) 648–653, https://doi.org/10.1016/j.ndteint.2010.06.010.

[21] A. Sophian, F. Nafiah, T. S. Gunawan, N. A. Mohd Yusof, and A. Al-Kelabi, "Machine-learning-based Evaluation of Corrosion Under Insulation in Ferromagnetic Structures," IIUM Eng. J., vol. 22, no. 2, pp. 226–233, Jul. 2021, 10.31436/iiumej.v22i2.1692.

[22] A. Sophian, G.Y. Tian, D. Taylor, J. Rudlin, A feature extraction technique based on principal component analysis for pulsed Eddy current NDT, NDT & E Int. 36 (1) (2003) 37–41.

[23] T. Chen, G.Y. Tian, A. Sophian, P.W. Que, Feature extraction and selection for defect classification of pulsed eddy current NDT, NDT E Int. 41 (6) (2008) 467–476.

[24] L. Bai, G. Yun Tian, A. Simm, S. Tian, Y. Cheng, Fast crack profile reconstruction using pulsed eddy current signals, NDT E Int. 54 (2013) 37–44, https://doi.org/10.1016/j.ndteint.2012.11.003.

[25] G.Y. Tian, Y. Li, C. Mandache, Study of Lift-Off Invariance for Pulsed Eddy-Current Signals, IEEE Trans. Magn. 45 (1) (Jan. 2009) 184–191, https://doi.org/10.1109/TMAG.2008.2006246.

[26] J. Bruna, S. Mallat, Invariant scattering convolution networks, IEEE Trans. Pattern Anal. Mach. Intell. 35 (8) (2013) 1872–1886, https://doi.org/10.1109/TPAMI.2012.230.

[27] W. Yang, K. Wang, W. Zuo, Neighborhood component feature selection for high-dimensional data, J. Comput. 7 (1) (2012) 162–168, https://doi.org/10.4304/jcp.7.1.161-168.

[28] C.E. Rasmussen, Gaussian processes in machine learning, in: in Summer school on machine learning, 2003, pp. 63–71.

[29] D.R. Jones, M. Schonlau, W.J. Welch, Efficient global optimization of expensive black-box functions, J. Glob. Optim. 13 (4) (1998) 455–492.

[30] N. Ulapane, A. Alempijevic, T. Vidal Calleja, J. Valls Miro, Pulsed Eddy Current Sensing for Critical Pipe Condition Assessment, Sensors 17 (10) (2017) 2208, https://doi.org/10.3390/s17102208.

[31] G. James, D. Witten, T. Hastie, R. Tibshirani, An introduction to statistical learning, vol. 112, Springer, 2017.

[32] P.-S. Huang, H. Avron, T.N. Sainath, V. Sindhwani, B. Ramabhadran, Kernel methods match deep neural networks on timit, in: in 2014 IEEE International Conference on Acoustics, Speech and Signal Processing (ICASSP), 2014, pp. 205–209.

[33] V. Kecman, T.-M. Huang, M. Vogt, Iterative single data algorithm for training kernel machines from huge data sets: Theory and performance, in: Support vector machines: Theory and Applications, Springer, 2005, pp. 255–274.

[34] J.H. Friedman, Greedy function approximation: a gradient boosting machine, Ann. Stat. (2001) 1189–1232.

[35] F.J. Massey, The Kolmogorov-Smirnov test for goodness of fit, J. Am. Stat. Assoc. 46 (253) (1951) 68–78.

[36] M.S. Bartlett, Probability, statistics and time: a collection of essays, Springer Science & Business Media, 2012.

[37] W.M. Mendenhall, T.L. Sincich, Statistics for Engineering and the Sciences, CRC Press, 2016.